Hindawi
Journal of Food Biochemistry
Volume 2024, Article ID 9445763, 14 pages
https://doi.org/10.1155/2024/9445763

Research Article

Integrating Network Pharmacology and Metabolomics to Explore the Potential Mechanism of Pinolenic Acid against Atherosclerosis

Zhanhong Cao,[1] **Zhuang Zhang**,[1] **Qing Yang**,[1] **Xingyu Fang**,[1] **Haonan Bai**,[1] **Hui Li**,[2] **Shifan Chen**,[3] **Dianyu Li**,[1] **Yu An**,[1] **Jian Liu**,[1] **Mengna Cheng**,[1] **Xin Sui**,[1] **and Na Li**[1]

[1]*Changchun University of Chinese Medicine, Changchun 130117, Jilin, China*
[2]*Qian Wei Hospital of Jilin Province, Changchun 130012, Jilin, China*
[3]*Department of Pathology, The Second Hospital of Jilin University, Changchun 130041, Jilin, China*

Correspondence should be addressed to Xin Sui; suixinmm@hotmail.com and Na Li; lina08@ccucm.edu.cn

Received 10 January 2023; Revised 6 December 2023; Accepted 28 December 2023; Published 6 January 2024

Academic Editor: Kandi Sridhar

Atherosclerosis (AS) is a global disease that causes a heavy economic burden and can significantly impact human health. Pinolenic acid (PLA) has antioxidant, anti-inflammatory, and lipid-lowering effects. However, it is unclear whether PLA holds a therapeutic promise for AS treatment or prevention. This study aims to investigate whether PLA can effectively treat AS and elucidate its therapeutic mechanism. To this end, potential PLA targets in AS treatment were identified by using network pharmacology. Additionally, an *in vitro* AS cell model was established by H_2O_2-induced damaging of human coronary artery endothelial cells (HCAECs). Subsequently, endothelial cell function was evaluated by evaluating cell proliferation, oxidative markers, reactive oxygen species (ROS), and nitric oxide (NO) levels. Cellular metabolomics was further employed to assess differential intracellular metabolites following H_2O_2 injury. In total, 87 overlapping target genes for PLA and AS were detected. PPI network analysis identified 38 hub genes closely associated with oxidative stress and fatty acid metabolism. Moreover, PLA improved cell survival and reduced oxidative stress injury by activating the NRF2/ARE signaling pathway *in vitro*. Cellular metabolomics confirmed that PLA might help maintain redox homeostasis and reduce endothelial cell injury by upregulating fatty acid β-oxidation. Taken together, our findings suggest that PLA prevents H_2O_2-induced HCAEC injury by maintaining redox homeostasis and may, therefore, represent a therapeutic potential for AS.

1. Introduction

Coronary artery disease (CAD) is a major cause of mortality worldwide, resulting in approximately 7.2 million deaths and costing 10 billion USD annually [1]. These statistics are anticipated to increase by approximately 18% and 43%, respectively, by 2030 [1]. Atherosclerosis (AS) is the most common underlying cause of CAD and is a chronic inflammatory and progressive pathophysiological process that damages the integrity of the arterial endothelium, resulting in atherosclerotic plaque formation [2]. Plaque formation is triggered by a series of events, involving endothelial dysfunction, uptake of LDL cholesterol into the arterial wall, inflammation with infiltration of immune cells, and proliferation and migration of vascular smooth muscle cells into the lesion [3]. Endothelial dysfunction is an early feature of AS that can lead to impaired anti-inflammatory properties of the endothelium, impaired regulation of vascular growth, and dysregulation of vascular remodeling, among other pathological conditions [4]. Endothelial cell (EC) dysfunction caused by the accumulation of ROS is closely correlated with the development and progression of AS [5, 6]. Furthermore, oxidative stress can induce EC apoptosis, ultimately leading to lipid homeostasis and immune dysregulation [7]. Therefore, it is essential to investigate the molecular mechanisms behind endothelial dysfunction for developing effective therapeutic strategies to combat AS. Although several chemical drugs can be used to treat AS, some of them exhibit serious side effects. Nevertheless, the extracts of natural products are relatively safe [8]. Moreover,

evidence suggests that replacing dietary saturated fatty acids with polyunsaturated fatty acids (PUFA) may prevent cardiovascular diseases [9, 10]. However, PUFA must be acquired from the diet or dietary supplements as humans are incapable of synthesizing the required levels *de novo* [11].

Pine nuts and pine nut oil (PNO) are classified as healthy foods in China and Japan. Their hypolipidemic effects are well documented within animal models [12]. PNO is rich in a variety of unusual delta-5-non-methylene-interrupted fatty acids (NMIFAs), which mainly include pinolenic acid (PLA; all cis-5, -9, -12 18 : 3), sciadonic acid (all cis-5, -11, -14 20 : 3), and taxoleic acid (all cis-5, -9 18 : 2) [13]. PLA is the most abundant of these NMIFAs in PNO, comprising 15%, and is a unique component of PNO [14]. Its chemical formula is $C_{18}H_{30}O_2$, which is the isomer of linolenic acid [15]. PLA is produced from linoleic acid (LA) via species-specific delta-5 desaturase [13]; in fact, its chemical structure is similar to that of γ-linolenic acid and α-linolenic acid (Figure 1). Siberian pine nuts and Korean pine nuts are abundant sources of PLA, containing up to 20% and 27% of their total content, respectively. PUFAs are also widely available in plant and marine sources. With diminishing fish stocks, plant-sourced PUFA may be a promising alternative to marine-sourced PUFA [16]. Thus, PLA may be a candidate as plant-derived PUFA and has various beneficial effects, including antioxidant, lipid-lowering, anti-inflammatory, and antidiabetic effects, as well as suppression of cancer cell invasion and motility [15, 17]. However, the action mechanism of PLA in AS by affecting endothelial function deserves further elucidation.

Herein, this study aimed to investigate the potential targets and pathways of PLA in AS by using network pharmacology. H_2O_2-treated human coronary artery endothelial cells (HCAECs) were used as an *in vitro* model of AS to elucidate whether PLA could protect HCAECs from H_2O_2-induced injury and to explore the mechanism of action by cellular metabolomics, which would provide a theoretical basis for the treatment of AS with PLA.

2. Materials and Methods

2.1. Network Pharmacology Analysis

2.1.1. Candidate Target Screening. The three-dimensional chemical structure of PLA was obtained from PubChem [18], and target genes related to PLA were determined from SwissTargetPrediction [19]. The AS-related genes were screened from the GeneCards [20], OMIM [21], and DrugBank [22] databases using the following keywords: "atherosclerosis," "arteriosclerosis," "atherogenesis," and "atheroscleroses." The overlapping PLA targets and AS targets were visualized using a Venn diagram with the online Bioinformatics tool.

2.1.2. Protein-Protein Interaction (PPI) Network Construction. The shared PLA and AS targets were entered into the STRING online database, and the minimum required interaction score was set at > 0.4 of mean medium confidence for PPI network establishment. The topological properties of the targets were evaluated with the CytoNCA tool to screen core targets highly connected to PLA against AS.

2.1.3. Enrichment Analysis. An investigation of Gene Ontology (GO) functional annotation and Kyoto Encyclopedia of Genes and Genomes (KEGG) pathway enrichment was conducted to further probe the potential mechanisms of PLA in AS therapy by using an online Metascape platform. The "Homo sapiens" setting was used to illustrate the biological processes of target genes in various clusters and their role in signal transduction. The top 25 correlated biological processes and KEGG pathways were graphed as a bubble diagram by using the online Bioinformatics Tools by P value ranking.

2.1.4. Target-Pathway Network Construction. The relationship between targets and signaling pathways was elucidated by introducing core target genes and the top 25 pathways into the online Bioinformatics Tools to construct a target-pathway (TP) network.

2.2. In Vitro Validation

2.2.1. Chemical Reagents. PLA (lot no. 2019112701, purity ≥ 99.8%) was obtained from Chengdu Pulis Biotechnology Co. Ltd. (Chengdu, China). Additional chemical reagents are displayed in supplementary.

2.2.2. Cell Culture and Treatments. HCAECs were provided by the Second Hospital of Jilin University, Jilin, China. The cells were cultured in high-glucose Dulbecco's modified Eagle's medium (Gibco) containing 10% fetal bovine serum (Clark) and 1% antibiotics (100 U/mL of penicillin and 100 mg/mL of streptomycin, HyClone) under standard culture conditions at 37°C and 5% CO_2. The medium was refreshed to remove nonadherent cells after a 24 h culture, and subsequent experiments were performed when the cells reached 70–80% confluency. Cells in the logarithmic growth phase were randomly classified into five groups: control, H_2O_2, low-dose PLA (PLAL), medium-dose PLA (PLAM), and high-dose PLA (PLAH). The PLAL, PLAM, and PLAH groups were pretreated with 5, 10, or 20 μM PLA, respectively, for 24 h, while the other two groups were pretreated with fresh culture medium for 24 h. The HCAECs in all treated groups were then incubated with H_2O_2 (400 μM) for 12 h, while the control group was incubated with an equivalent volume of culture medium for 12 h.

2.2.3. Cell Viability Assay. HCAECs were seeded into 96-well plates at a density of 5×10^4 cells/well, and the above-mentioned treatments were performed. MTT (20 μL, 5 mg/mL) was added and incubated at 37°C for 4 h. Subsequently, 150 μL of DMSO was added to each well with shaking for 10 min at 37°C. Absorbance was recorded by using a microplate reader (Tecan, Switzerland) at 490 nm.

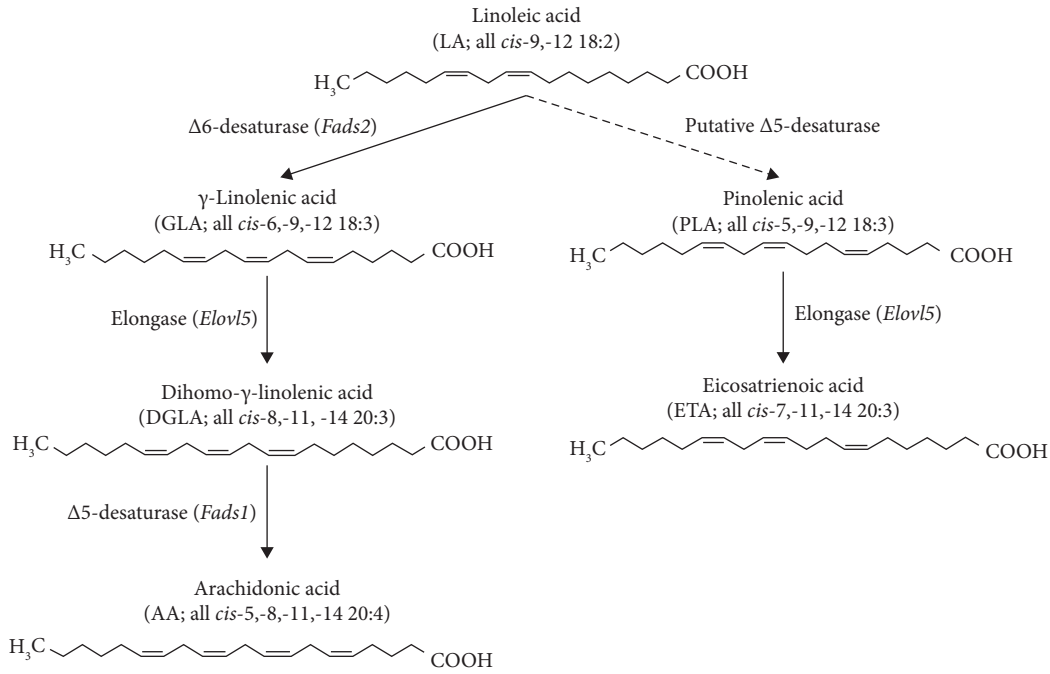

Figure 1: The pathway of conversion of linoleic acid to γ-linolenic, dihomo-γ-linolenic, arachidonic, pinolenic, and eicosatrienoic acids.

2.2.4. Real-Time Cellular Analysis (RTCA). An empty medium was added to E-Plate16 to determine the baseline. The cells were then seeded into E-Plate16 at 5×10^4 cells/well in 100 μL/well (two replicates per concentration). The E-Plate16 was placed into the instrument to obtain the cell growth curve, and cells in the logarithmic growth phase were treated as described in Section 2.2.2. Cell-drug interactions were determined according to the growth curves automatically generated by the instrument.

2.2.5. Detection of Lipid Peroxidation and NO Levels. The cellular ROS, GSH, and MDA contents and SOD and CAT activities were examined according to the manufacturer's recommendations to comprehensively evaluate the degree of lipid oxidation damage in cells. The NO content of the cell supernatant was also determined following the manufacturer's instructions.

2.2.6. Determination of the FFA and ATP Content. These values were detected based on the manufacturer's instructions.

2.2.7. Immunofluorescence Assay. Immunofluorescence assays were performed as previously described [23]. In brief, after the cells were fixed and permeabilized, they were incubated with the p-NRF2 antibody overnight at 4°C, followed by incubation with fluorescently-labeled secondary antibodies for 1 h at 37°C and DAPI for 5 min at 37°C to stain the nuclei. Photographs were obtained and observed by using a laser confocal microscope (Olympus, Japan).

2.2.8. Cellular Metabolomics Analysis. Data related to cellular metabolite extraction, LC-MS/MS analysis, and data preprocessing and annotation are listed in supplementary. HCAEC was randomly assigned to three groups: control, H_2O_2, and PLAH. Cells in the logarithmic growth phase were treated as described in Section 2.2.2. Cellular metabolites were extracted and subjected to LC/MS analysis.

2.2.9. Western Blotting Analysis. Cells were lysed in ice-cold RIPA buffer, and the total protein was extracted. Protein (20 μg) was separated on a 10% SDS-PAGE gel and transferred to a PVDF membrane (Millipore Co., Ltd. USA). The membrane was blocked with 5% skim milk at 37°C for 2 h and incubated overnight at 4°C with primary antibodies against ET-1, NRF2, p-NRF2, KEAP1, AARE, HO-1, PPARα, CPT1α, ACC, or β-actin. The membranes were washed with TBST and incubated with a secondary antibody at 37°C for 1 h. The signal intensity of the protein bands was observed by using a chemiluminescence imaging system, and the gray values of the protein bands were quantified by Image J software (NIH, Bethesda, MD, USA).

2.2.10. Statistical Analysis. Data were analyzed in GraphPad Prism 8 (GraphPad Software, San Diego, CA, USA) and were presented as the mean ± standard deviation (SD) of continuous variables. Student's t-test was performed to assess the statistical significance of comparisons between the two groups, and one-way analysis of variance (ANOVA) was used for comparisons among multiple groups. $P < 0.05$ was considered statistically significant.

3. Results

3.1. Screening of Candidate Targets. A total of 109 PLA-related targets were identified based on the SwissTargetPrediction database. The OMIM, GeneCards, and

DrugBank databases indicated that 4,892 genes were associated with AS. Moreover, 87 common targets were obtained by the Venn diagram as potential targets of PLA in the treatment of AS (Figure 2(a)).

3.2. PPI Network Construction and Analysis. A PPI network was constructed to better understand the protein-protein interactions. The 87 overlapping targets were entered into the STRING database to establish a PPI network. The initial PPI network was introduced into Cytoscape 3.8.2 for visualization (Figure 2(b)) and was estimated centrally by using the CytoNCA plugin. The degree value served as an indicator of the contribution made by PLA to AS, that is, the higher the degree value, the more biologically relevant the target. A total of 38 targets with a degree value of more than the median (7) were recognized as key targets, including PPARG, PTGS2, PPARA, MAPK1, ESR1, PLA2G4A, ALOX5, BCL2L1, PTGS1, and PTGES (Figure 2(c)). This network comprised 38 nodes and 195 edges.

3.3. Enrichment Analysis. A total of 503 biological processes (BP), 32 cellular components (CC), and 61 molecular functions (MF) were enriched. BP was associated with fatty acid metabolic processes, unsaturated fatty acid biosynthetic processes, and regulation of inflammatory responses (Figure 3(a)). The associated CC included the organelle outer membrane, outer membrane, and nuclear envelope (Figure 3(b)). The most enriched MF were related to oxidoreductase activity, acting on single donors with incorporation of molecular oxygen, incorporation of two atoms of oxygen, ligand-activated transcription factor activity, and nuclear receptor activity (Figure 3(c)). The KEGG pathway enrichment further revealed that critical pathways are enriched in arachidonic acid metabolism, PPAR signaling pathway, and pathways in cancer (Figure 3(d)). The top 25 BP, CC, MF, and KEGG pathway terms were ordered by P value (Figures 3(a)–3(d)).

3.4. TP Network Analysis of PLA against AS. A total of 38 hub targets and 25 signaling pathways were identified (Figure 4). Taken together, these results confirm that PLA plays a protective role in the treatment of AS through multiple pathways and targets.

3.5. Effect of PLA on Cell Viability. HCAEC proliferation at densities of 1×10^5 cells/mL, 5×10^4 cells/mL, 2.5×10^4 cells/mL, and 1×10^4 cells/mL was monitored by using RTCA. The slope of the proliferation curve significantly increased and peaked at approximately 40 h when the HCAEC density was 5×10^4 cells/mL. Hence, this density was selected for subsequent experiments (Figure S2). Cells were treated with 100–600 μM H_2O_2 for 6, 12, or 24 h, and the cell viability decreased in a dose-dependent manner. Subsequently, H_2O_2 (400 μM, 12 h) was applied to establish a cell-injury model (Figure S3). Incubation of HCAEC with 0–50 μM of PLA for 24 h had no conspicuous inhibitory effect on cell growth (Figure S4). Interestingly, pretreatment with PLA at 5, 10, or 20 μM for 24 h, followed by incubation with 400 μM of H_2O_2 for 12 h, increased cell viability (Figures 5(a) and S5), which was confirmed by using RTCA (Figure 5(b)). These results suggest that PLA (5, 10, and 20 μM) protects HCAEC from H_2O_2-induced cell injury. In subsequent experiments, HCAEC were pretreated with PLA (5, 10, and 20 μM) for 24 h before H_2O_2 (400 μM) exposure for 12 h.

3.6. Effect of PLA on Lipid Peroxidation Injury and NO Levels. We measured the contents of ROS, GSH, and MDA and the activities of SOD and CAT to assess the protective effect of PLA on HCAEC stimulated by H_2O_2. Compared with those in the control group, the ROS and MDA contents in the H_2O_2 group were significantly increased, whereas that of GSH and the activities of SOD and CAT were significantly decreased (Figures 6(a)–6(e)). Meanwhile, PLA pretreatment significantly decreased the ROS and MDA contents and increased GSH and the activities of SOD and CAT compared with the H_2O_2 group. The NO level significantly decreased in the H_2O_2 group, whereas PLA pretreatment increased NO levels (Figure 6(f)). These results indicate that PLA pretreatment alleviates oxidative stress injury and increases NO levels.

3.7. Effect of PLA on FFA and ATP Contents. FFA levels were higher and ATP levels were lower in the H_2O_2 group than in the control group (Figure 7). PLA pretreatment significantly decreased FFA levels and increased ATP levels compared with the H_2O_2 group.

3.8. Metabolomic Analysis of HCAEC Treated with PLA. Disease states can cause changes in cell metabolism, and metabolite composition can reveal dysfunction in physiological and pathological states [24]. The total ion chromatogram for each sample is presented in Figure S1. Accordingly, the metabolic profiles of the cells in each group were compared and analyzed by using a principal component analysis (PCA) score plot ($R^2X = 0.561$) (Figure 8(a)). The control group was significantly separated from the H_2O_2 group, confirming the successful establishment of the cell model. Compared with the H_2O_2 group, the PLA group was able to "callback" a metabolic profile that resembled that of the control group and differed from the H_2O_2 group. OPLS-DA was used to select more reliable differential metabolites between groups, analyze the control and H_2O_2 groups, and distinguish the differential metabolites with a significant separation between these groups ($R^2X = 0.647$, $R^2Y = 1$, *and* $Q^2 = 0.92$; Figure 8(b)). The permutation test showed that the model was not overfitted, and the data collected from the model could be applied for further analysis (Figure 8(c)).

Finally, 108 differentially abundant endogenous metabolites with VIP >1 and $P < 0.05$ were identified in the H_2O_2 group (Tables S1 and S2). The abundance of eight differential metabolites reverted to normal levels after PLA treatment (Table 1, Figure S6). The heatmap of the differential metabolite quantification data showed that the levels

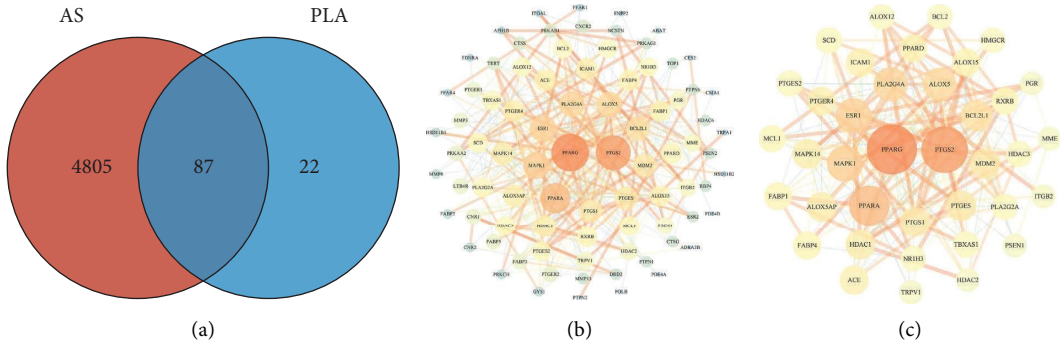

Figure 2: Network pharmacological analysis of PLA in AS. (a) Venn diagram of the common targets of PLA in AS. (b) PPI network of PLA against AS (87 common targets). (c) PPI network of PLA against AS (38 hub targets).

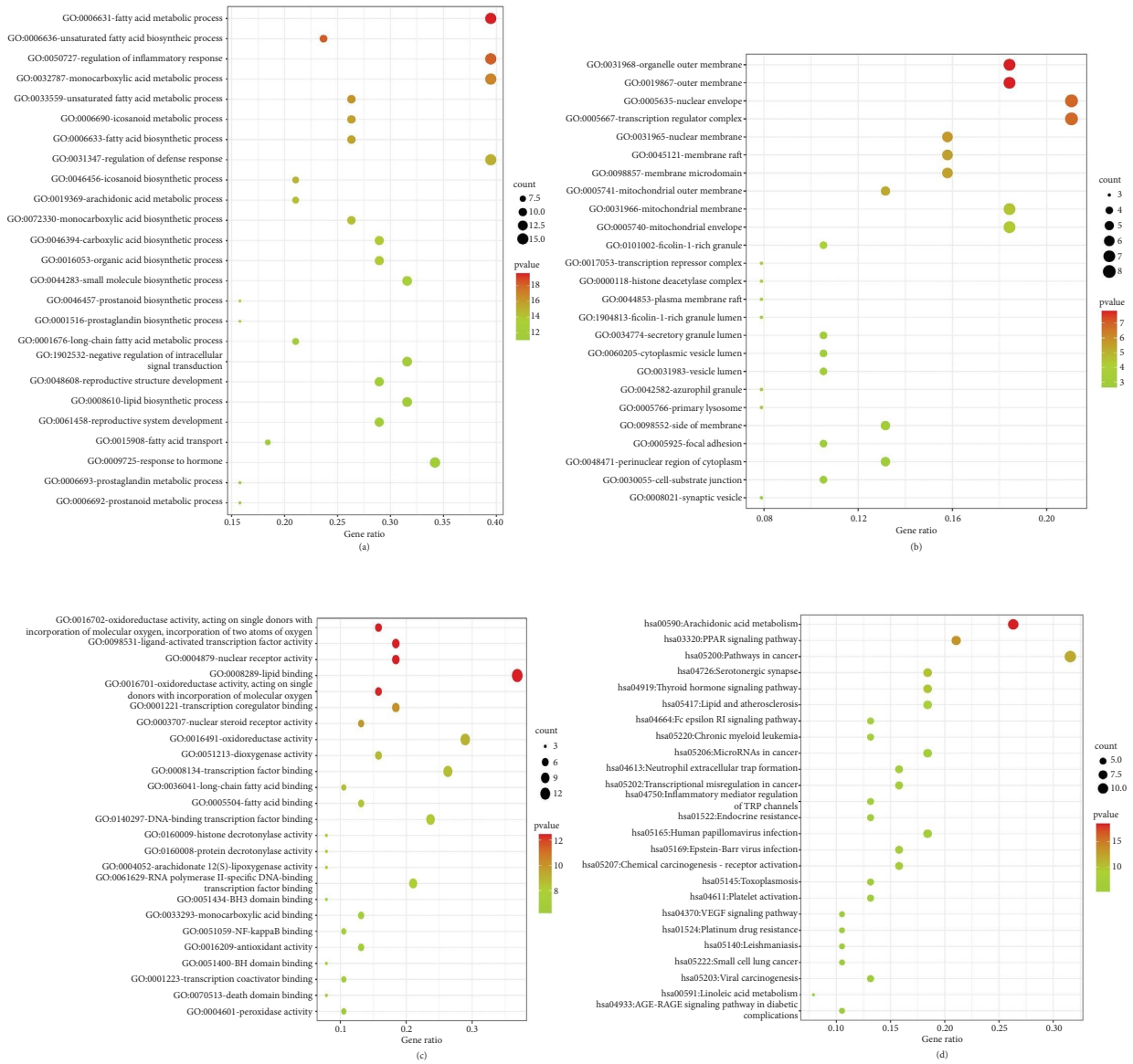

Figure 3: Bubble diagram of GO enrichment analysis and KEGG enrichment pathway analysis of PLA-AS genes. The top 25 GO entries for biological processes (BP) (a), cellular components (CC) (b), molecular functions (MF) (c), and KEGG pathways (d).

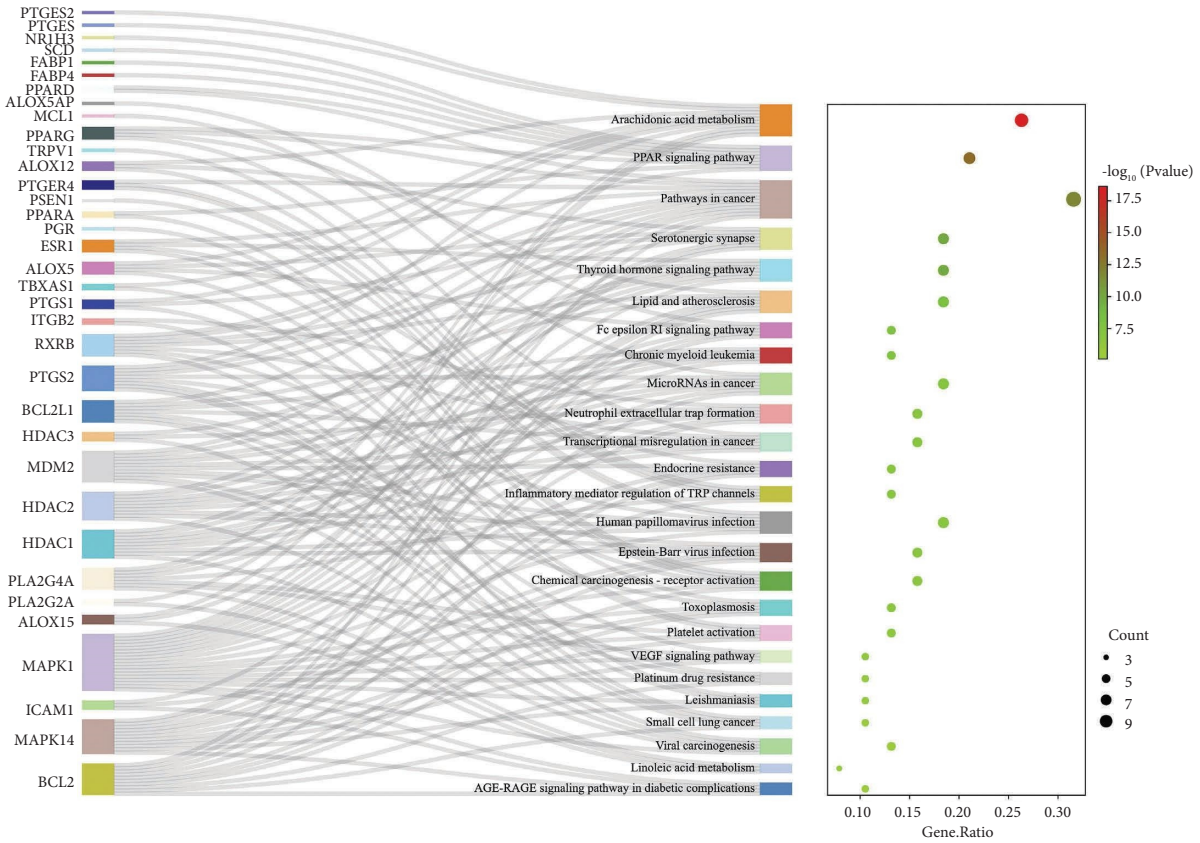

Figure 4: TP networks of PLA in the treatment of AS.

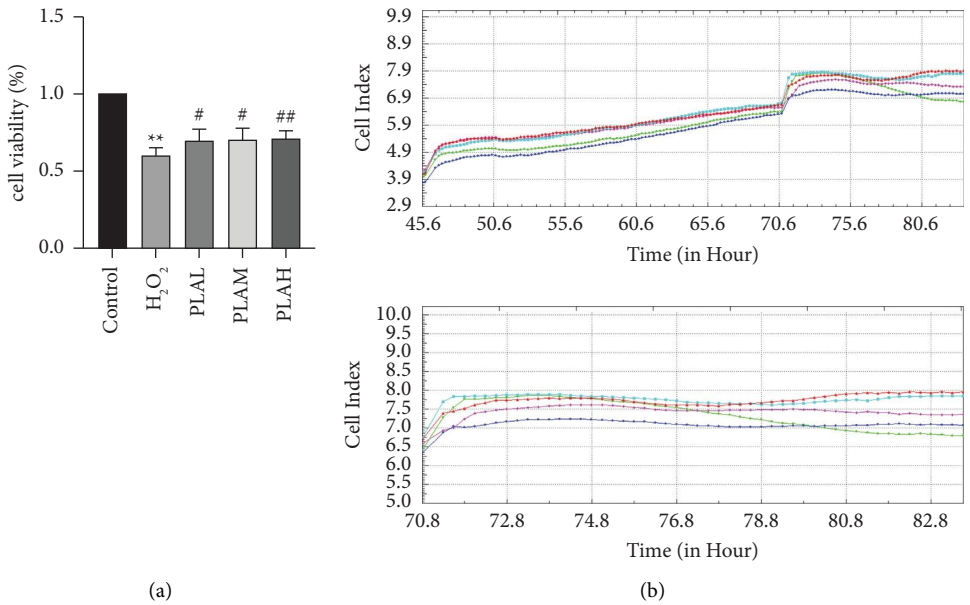

(a) (b)

Figure 5: Effect of PLA on cell viability. (a) Cell viability at different PLA concentrations. (b) Cell growth curve (red: control; green: H_2O_2; blue: PLAL; purple: PLAM; cyan: PLAH). Data are expressed as the mean ± SD. $^{**}P < 0.01$ versus the control group; $^{\#}P < 0.05$, $^{\#\#}P < 0.01$ versus the H_2O_2 group.

of creatinine and succinic acid semialdehyde significantly increased in the PLA group compared with those in the H_2O_2 group (Figure 8(d)). Meanwhile, the levels of arachidonic acid (AA), oleic acid (OA), LA, ethyl oleate (EO), sclareol, and docosahexaenoic acid (DHA) significantly decreased.

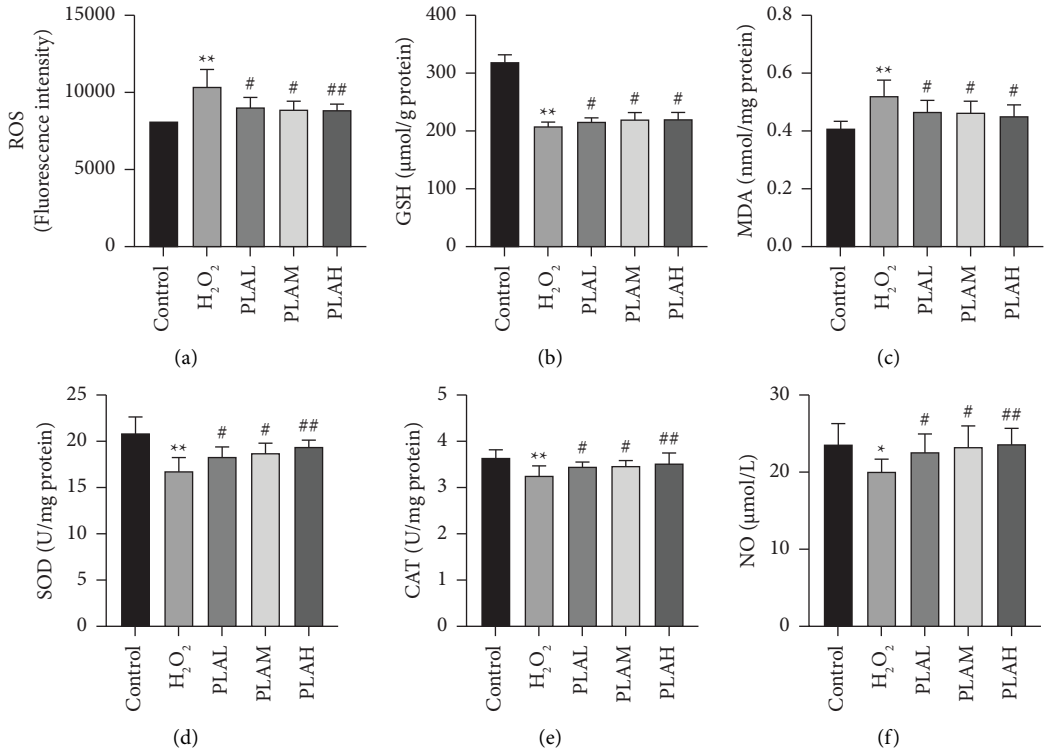

Figure 6: Effect of PLA on lipid peroxidation injury and NO content. Levels of ROS (a), GSH (b), MDA (c), and NO (f), and activity of SOD (d) and CAT (e). Data are expressed as mean ± SD. $^{*}P < 0.05$, $^{**}P < 0.01$ versus the control group; $^{\#}P < 0.05$, $^{\#\#}P < 0.01$ versus the H_2O_2 group.

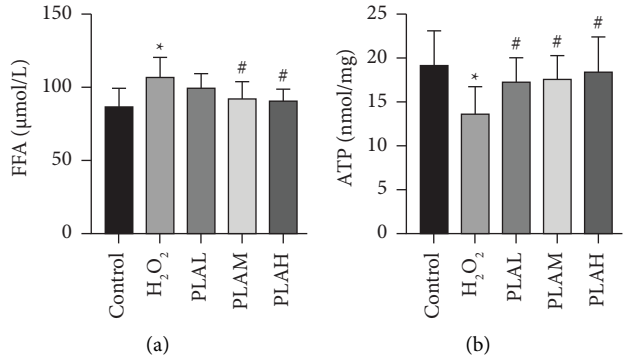

Figure 7: Effect of PLA on the FFA (a) and ATP (b) content. Data are expressed as the mean ± SD. $^{*}P < 0.05$ versus the control group; $^{\#}P < 0.05$ versus the H_2O_2 group.

Differentially abundant metabolite information was input into MetaboAnalyst 5.0 to perform metabolic pathway analysis. PLA may elicit its protective effect by interfering with LA metabolism, Alanine, aspartate and glutamate metabolism, Butanoate metabolism, AA metabolism, and Arginine and proline metabolism (Figure 8(e)). Interestingly, KEGG pathway analysis showed that AA metabolism and LA metabolism were enriched. The results suggested that the protective effect elicited by PLA in H_2O_2-injured HCAEC might be associated with AA metabolism and LA metabolism regulation.

3.9. Effect of PLA on Expression of NRF2/ARE Signaling Pathway-Related Proteins and ET-1 Protein. The NRF2/ARE signaling pathway is one of the most critical endogenous antioxidant pathways. Increased ET-1 expression promotes the development of AS [25]. As such, the expression of proteins associated with this pathway was evaluated in HCAEC. Compared to that in the control group, the expression of NRF2, p-NRF2, AARE, and HO-1 was significantly decreased in the H_2O_2 group, while that of KEAP1 and ET-1 was significantly increased (Figures 9(a) and 9(b)

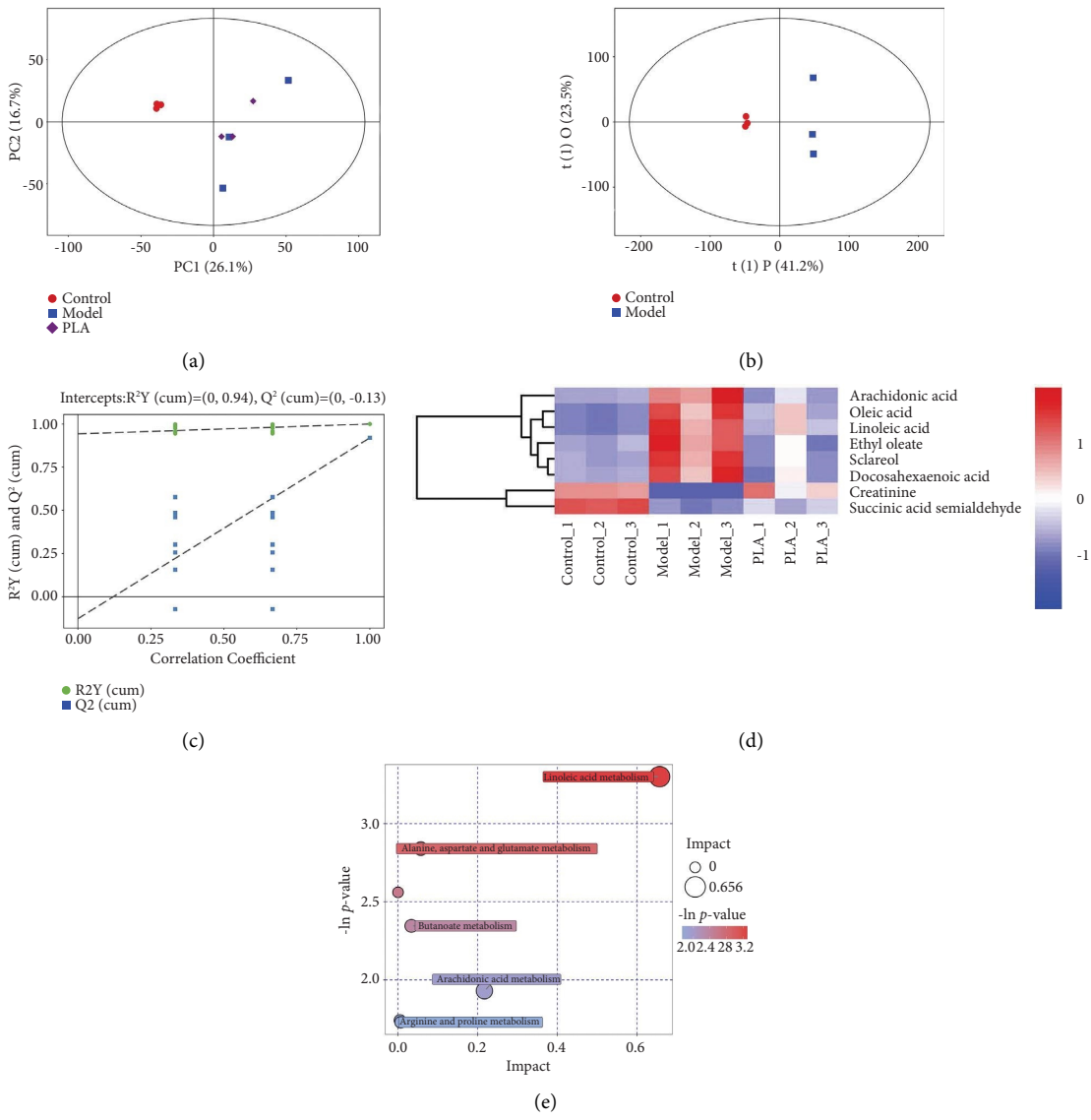

Figure 8: Effects of PLA on HCAEC metabolites. (a) Principal component analysis score plot from the control, model, and PLA groups. (b, c) Orthogonal partial least squares discriminant analysis score plot and permutation test between the control and model groups. (d) Metabolite hierarchical clustering analysis. Blue indicates downregulation and red represents upregulation. The darker the color, the larger the difference. (e) Overview of metabolic pathways modified by PLA.

Table 1: Differential metabolites in H_2O_2-induced HCAEC injury and the trends in the changes between each pair of groups.

RT (s)	Metabolites	HMDB	Formula	H_2O_2 vs control		PLA vs H_2O_2	
				Trend	FC	Trend	FC
36.385	Linoleic acid	HMDB0000673	$C_{18}H_{32}O_2$	$\uparrow^{*}$	1.899	$\downarrow^{\#}$	0.683
36.134	Sclareol	HMDB0036827	$C_{20}H_{36}O_2$	$\uparrow^{*}$	2.028	$\downarrow^{\#}$	0.515
36.386	Oleic acid	HMDB0000207	$C_{18}H_{34}O_2$	$\uparrow^{*}$	2.055	$\downarrow^{\#}$	0.647
36.200	Arachidonic acid	HMDB0001043	$C_{20}H_{32}O_2$	$\uparrow^{*}$	2.456	$\downarrow^{\#}$	0.428
36.200	Ethyl oleate	HMDB0034451	$C_{20}H_{38}O_2$	$\uparrow^{**}$	1.813	$\downarrow^{\#}$	0.561
36.167	Docosahexaenoic acid	HMDB0002183	$C_{22}H_{32}O_2$	$\uparrow^{*}$	1.903	$\downarrow^{\#}$	0.541
176.319	Creatinine	HMDB0000562	$C_4H_7N_3O$	$\downarrow^{***}$	0.0002	$\uparrow^{\#}$	3729.156
180.546	Succinic acid semialdehyde	HMDB0001259	$C_4H_6O_3$	$\downarrow^{***}$	0.231	$\uparrow^{\#}$	1.657

$^{*}P < 0.05$, $^{**}P < 0.01$, $^{***}P < 0.001$ versus the control group; $^{\#}P < 0.05$ versus the H_2O_2 group.

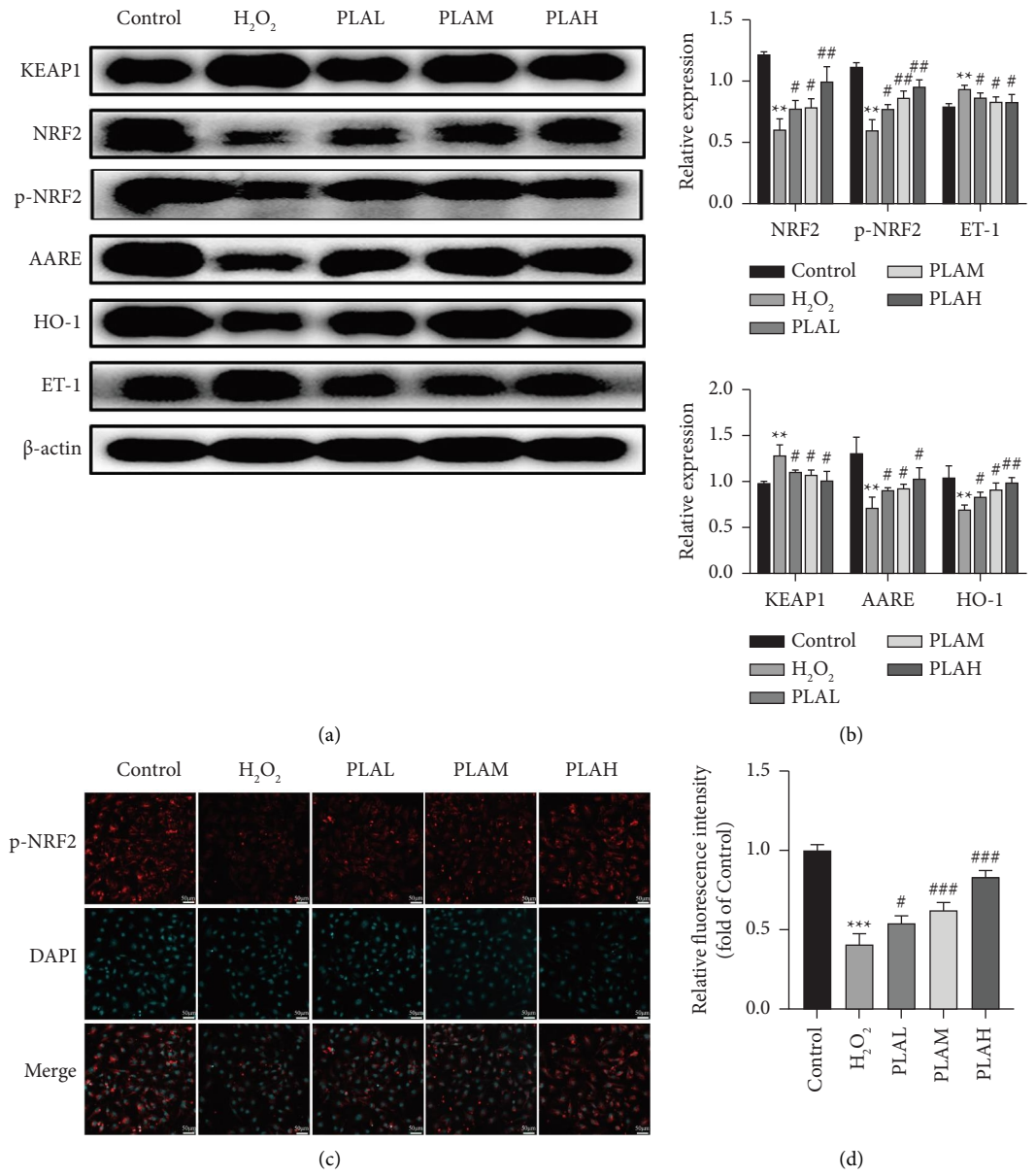

Figure 9: Effect of PLA on the levels of proteins associated with the NRF2/ARE signaling pathway and ET-1 protein. (a) Protein levels. (b) Quantified protein expression levels. β-Actin was used as an internal control. (c) Immunofluorescence of p-NRF2 (p-NRF2-AF594; nucleus stained with DAPI). Scale bar = 50 μm. (d) Relative fluorescence intensity of p-NRF2. Data are expressed as the mean ± SD. $^{**}P < 0.01$, $^{***}P < 0.001$ versus the control group; $^{\#}P < 0.05$, $^{\#\#}P < 0.01$, $^{\#\#\#}P < 0.001$ versus the H_2O_2 group.

and S7). PLA pretreatment significantly increased the expression of NRF2, p-NRF2, AARE, and HO-1 while decreasing that of KEAP1 and ET-1 compared to the H_2O_2 group. Moreover, immunofluorescence results confirmed that PLA treatment increased the expression of p-NRF2 and promoted nuclear translocation (Figures 9(c) and 9(d)). These results indicate that PLA pretreatment enhances the antioxidant defense mechanism of HCAEC and decreases ET-1 expression.

3.10. Effect of PLA on the Expression of Fatty Acid Metabolism-Related Proteins. The integration of network pharmacology and cellular metabolomics results revealed that PLA may protect HCAEC by regulating LA metabolism and AA metabolism, both of which are associated with FA metabolism. Therefore, we assessed the expression of PPARα, CPT1α, and ACC. Compared with that in the control group, the expression of PPARα and CPT1α decreased in the H_2O_2 group, while that of ACC increased (Figures 10 and S8).

However, PLA pretreatment significantly increased PPARα and CPT1α expression and decreased ACC expression compared with the H_2O_2 group. These findings further support the notion that PLA pretreatment improves FA metabolism.

4. Discussion

Endothelial dysfunction is related to the development and progression of AS [26]. Therefore, improving endothelial function may be an effective method for AS treatment [7]. Growing evidence has confirmed that H_2O_2-induced oxidative stress contributes to endothelial dysfunction [27]. Thus, the H_2O_2-induced HCAECs injury model can serve as a suitable *in vitro* model to explore the mechanisms of EC injury and AS [28].

Network pharmacology has become a promising approach for drug discovery and development, particularly in traditional Chinese medicine (TCM) investigations. This approach provides a novel network model of "multitarget, multieffect, and complex disease," which is compatible with the nature of TCM and its holistic concept [29]. In this study, we first identified the target proteins of PLA by using network pharmacology analysis. Then, we constructed a TP network to predict the mechanisms of PLA. The AA, LA, and PPARα signaling pathways were tentatively identified as the mechanisms by which PLA exerts its anti-AS effects based on GO and KEGG pathway enrichment analyses and existing literature reports. Given that AA and LA metabolisms significantly stimulate ROS generation leading to oxidative stress [30, 31], the protective effects of PLA are likely related to oxidative stress.

We found that PLA pretreatment significantly increased GSH and NO levels and SOD and CAT activities while reducing ROS and MDA levels. ROS levels and NO bioavailability are critical regulatory factors of EC function, and their imbalance leads to endothelial dysfunction [32]. Excessive ROS production leads to lipid peroxidation, which suppresses the activity of antioxidant enzymes, including SOD, GSH, and CAT. Meanwhile, the MDA level reflects the degree of oxidative stress. Endothelium-derived NO exerts antioxidant and antiapoptotic effects in ECs to elicit an anti-AS effect [33]. Indeed, endothelial dysfunction is closely related to the decreased bioavailability of NO due to reduced NO generation in EC or increased inactivation of NO by ROS [34, 35].

We also revealed that PLA significantly increased the abundances of NRF2, p-NRF2, AARE, and HO-1 while inhibiting those of KEAP1 and ET-1. NRF2 is a key transcription factor that contributes to antioxidant stress regulation. Under normal physiological conditions, NRF2 is localized in the cytoplasm and is continuously degraded through KEAP1 ubiquitination [36]. However, oxidative stress leads to NRF2 dissociation from KEAP1, enabling NRF2 accumulation and phosphorylation in the cytoplasm. Phosphorylated NRF2 then translocates to the nucleus where it dimerizes with small Maf proteins and recognizes ARE sequences, promoting the transcription of antioxidant genes, such as *HO-1* and *SOD* [37]. One study revealed that extraordinary intensities of oxidative stress led to NRF2 downregulation [38]. Meanwhile, another study confirmed that H_2O_2 prevented the nuclear translocation of p-NRF2 and its expression [39]. HO-1 can scavenge ROS to prevent excessive lipid and protein oxidation, thus performing a potent antioxidant role [40]. Moreover, AARE is essential in the scavenging of oxidatively damaged proteins, contributes to the repair of single-stranded DNA breaks following cellular damage, and enhances the survival rate of cells exposed to ROS [41]. ET-1 functions as a powerful vasoconstrictor that induces increased ROS production in the vasculature, leading to eNOS uncoupling, decreased NO bioavailability, and endothelial dysfunction [42]. Taken together, these data suggest that PLA activates the NRF2/ARE signaling pathway and decreases ET-1 expression.

Endothelial dysfunction triggered by elevated FA levels also plays a key role in AS initiation and development [43]. Metabolomic results showed that PLA exerts a protective effect by significantly increasing the levels of creatinine and succinic acid semialdehyde while decreasing those of AA, OA, LA, EO, sclareol, and DHA. These eight metabolites were most enriched in LA metabolism, butanoate metabolism, and AA metabolism. Oxidized LA metabolites play a central role in the pathogenesis of AS. LA can also be elongated to AA, which is further synthesized into various proinflammatory mediators, such as leukotrienes and prostaglandins [44]. Excessive FFA contributes to incomplete oxidation of the mitochondria causing ROS production, whereas LA can generate greater mitochondria-derived ROS than FFA [31]. AA is one of the most abundant and widely circulated PUFA in living organisms [45]. It plays a critical role in inflammation, is associated with oxidative stress, and can promote high ROS production through various pathways [30]. Similarly, OA is a common monounsaturated FA that induces a cytotoxic response called "lipotoxicity," regulated by increased ROS levels or oxidative stress. An animal study showed that OA can lead to increased H_2O_2 levels, which are closely related to AS progression [46]. DHA is a major component of the phospholipid membrane and participates in membrane fluidity and signal transduction [47]. However, DHA can also cause disorder in the surrounding lipids due to rapid isomerization, leading to enhanced mobility, and keeps cholesterol out of distinct cholesterol domains [48]. EO is an ester of OA and is often associated with cholesteryl esters and triglycerides [49]. OA can injure the mitochondria and induce apoptosis through oxidative stress [50]. Sclareol can also induce apoptosis through the activation of mitochondrial and death receptor pathways [51]. Creatinine levels positively correlate with endothelial function [52]. Decreased production of succinic acid semialdehyde may lead to low levels of succinate, further contributing to the dysfunction of the tricarboxylic acid cycle [53]. Notably, AA metabolism and LA metabolism were also enriched, as revealed by KEGG pathway analysis. Moreover, examination of the crucial factors involved in FA metabolism confirmed that inhibition of EC FA β-oxidation (FAO) reduces the level of NADPH and increases the ratio of $NADP^+$/NADPH, causing oxidative stress and EC injury [54]. Meanwhile,

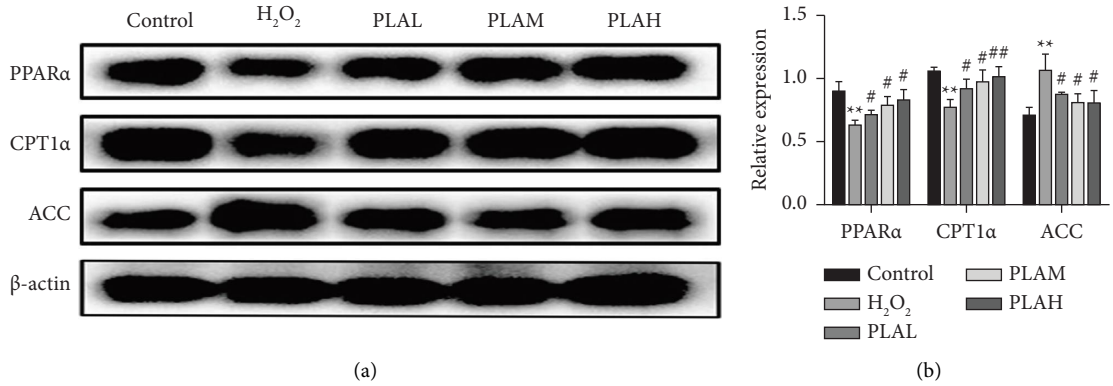

FIGURE 10: Effect of PLA on the expression of fatty acid metabolism-related proteins. (a) Protein levels. (b) Quantified protein expression levels. β-actin was used as an internal control. Data are expressed as mean ± SD. $^{**}P < 0.01$ versus the control group; $^{\#}P < 0.05$, $^{\#\#}P < 0.01$ versus the H_2O_2 group.

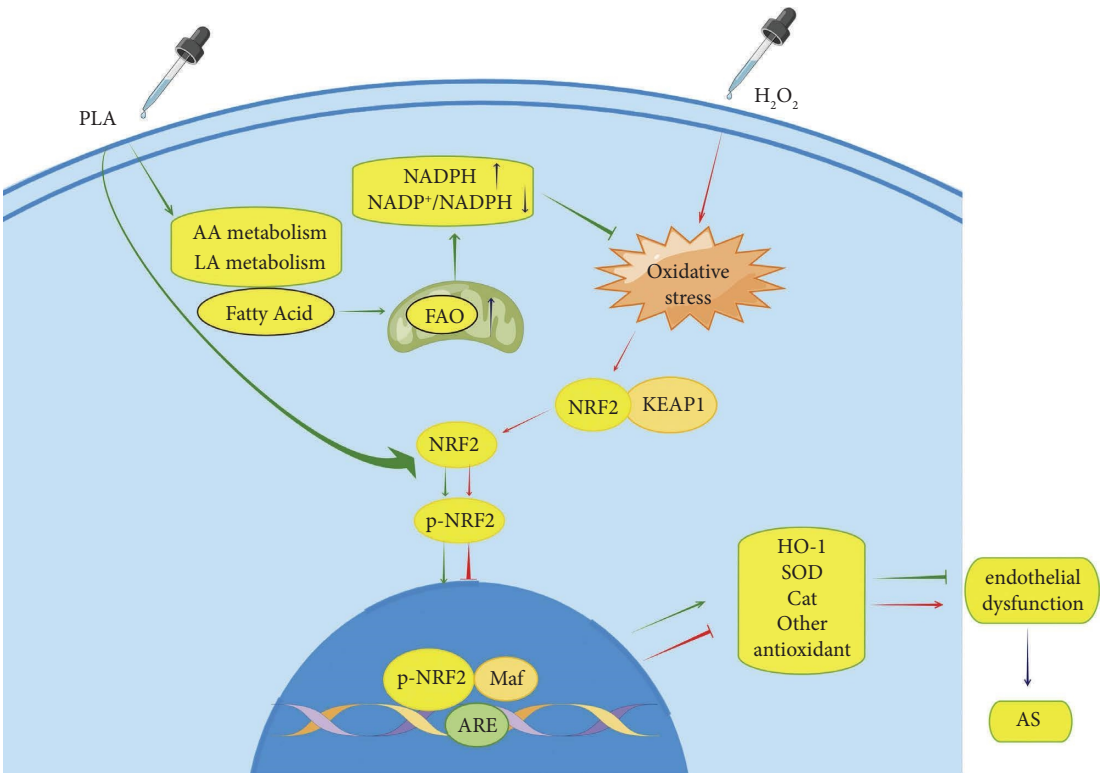

FIGURE 11: Schematic representation of the potential protective mechanism of PLA on H_2O_2-induced HCAEC injury by maintaining redox homeostasis.

NRF2 activation can improve FAO [55]. PLA pretreatment also significantly increased the expression of PPARα and CPT1α while decreasing that of ACC. PPARα activation can upregulate mitochondrial FAO and promote FA catabolism [56]. In contrast, ACC activation can promote FA synthesis and inhibit FAO [57]. FA is transported to the mitochondria by the rate-limiting enzyme CPT1α; and this is critical for FAO [58].

In summary, this study integrated network pharmacology and metabolomics to explore the potential mechanism of PLA in the treatment of AS. We revealed that PLA may attenuate H_2O_2-induced HCAEC injury by activating the NRF2/ARE signaling pathway and upregulating FAO (Figure 11). This finding provides a promising alternative therapeutic strategy for AS.

Data Availability

The data used to support the findings of this study are available from the corresponding author upon request.

Conflicts of Interest

The authors declare that they have no conflicts of interest regarding the publication of this paper.

Authors' Contributions

Zhanhong Cao and Zhuang Zhang contributed equally to this study. All authors read and approved the final manuscript.

Acknowledgments

This research was funded by Jilin Province Health and Healthy Youth Science and Technology Backbone Training Program Project (Grant no. 2020Q049).

Supplementary Materials

Supplementary Materials: 1) Chemical reagent. 2) Cellular metabolites extraction, LC-MS/MS analysis, and data preprocessing and annotation. Figure S1: TIC of each sample. Figure S2: Growth curve of HCAEC with different densities. Figure S3: Effects of different concentrations of H_2O_2 on the survival rate of HCAEC cells. Figure S4: Effects of different concentrations of PLA on the survival rate of HCAEC cells. Figure S5: Effect of different doses and times of PLA on the survival rate of HCAEC cells injured by H_2O_2. Figure S6: Metabolites hierarchical clustering analysis. Figure S7: Original data of western blotting of NRF2/ARE signaling pathway-related proteins and ET-1 protein. Figure S8: Original data of western blotting of fatty acid metabolism-related proteins. Table S1 and S2: Metabolomic analysis of HCAEC cells treated with PLA. (*Supplementary Materials*)

References

[1] E. K. Valanti, K. Dalakoura-Karagkouni, P. Fotakis et al., "Reconstituted HDL-apoE3 promotes endothelial cell migration through ID1 and its downstream kinases ERK1/2, AKT and p38 MAPK," *Metabolism*, vol. 127, Article ID 154954, 2022.

[2] M. G. Kiss and C. J. Binder, "The multifaceted impact of complement on atherosclerosis," *Atherosclerosis*, vol. 351, pp. 29–40, 2022.

[3] M. Grootaert and M. Bennett, "Sirtuins in atherosclerosis: guardians of healthspan and therapeutic targets," *Nature Reviews Cardiology*, vol. 19, no. 10, pp. 668–683, 2022.

[4] X. Shi, Y. Guan, S. Jiang, T. Li, B. Sun, and H. Cheng, "Renin-angiotensin system inhibitor attenuates oxidative stress induced human coronary artery endothelial cell dysfunction via the PI3K/AKT/mTOR pathway," *Archives of Medical Science*, vol. 15, no. 1, pp. 152–164, 2019.

[5] R. M. Touyz, A. Anagnostopoulou, F. Rios, A. C. Montezano, and L. L. Camargo, "NOX5: molecular biology and pathophysiology," *Experimental Physiology*, vol. 104, no. 5, pp. 605–616, 2019.

[6] Y. Joe, M. J. Uddin, J. Park et al., "Chung Hun Wha Dam Tang attenuates atherosclerosis in apolipoprotein E-deficient mice via the NF-κB pathway," *Biomedicine and Pharmacotherapy*, vol. 120, Article ID 109524, 2019.

[7] B. Zhang, Z. Hao, W. Zhou et al., "Formononetin protects against ox-LDL-induced endothelial dysfunction by activating PPAR-γ signaling based on network pharmacology and experimental validation," *Bioengineered*, vol. 12, no. 1, pp. 4887–4898, 2021.

[8] K. K. Oh, M. Adnan, and D. H. Cho, "A network pharmacology analysis on drug-like compounds from Ganoderma lucidum for alleviation of atherosclerosis," *Journal of Food Biochemistry*, vol. 45, no. 9, Article ID e13906, 2021.

[9] K. Pigsborg, G. Gürdeniz, O. D. Rangel-Huerta, K. B. Holven, L. O. Dragsted, and S. M. Ulven, "Effects of changing from a diet with saturated fat to a diet with n-6 polyunsaturated fat on the serum metabolome in relation to cardiovascular disease risk factors," *European Journal of Nutrition*, vol. 61, no. 4, pp. 2079–2089, 2022.

[10] F. H. Chilton, A. Manichaikul, C. Yang et al., "Interpreting clinical trials with Omega-3 supplements in the context of ancestry and FADS genetic variation," *Frontiers in Nutrition*, vol. 8, Article ID 808054, 2021.

[11] R. Gopalam, V. Manasa, S. R. Vaishnav, P. Daga, and A. W. Tumaney, "Profiling of lipids, nutraceuticals, and bioactive compounds extracted from an oilseed rich in PUFA," *Plant Foods for Human Nutrition*, vol. 77, no. 1, pp. 98–104, 2022.

[12] J. Zhang, S. D. Zhang, P. Wang et al., "Pinolenic acid ameliorates oleic acid-induced lipogenesis and oxidative stress via AMPK/SIRT1 signaling pathway in HepG2 cells," *European Journal of Pharmacology*, vol. 861, Article ID 172618, 2019.

[13] E. J. Baker, E. A. Miles, and P. C. Calder, "A review of the functional effects of pine nut oil, pinolenic acid and its derivative eicosatrienoic acid and their potential health benefits," *Progress in Lipid Research*, vol. 82, Article ID 101097, 2021.

[14] A. R. Lee and S. N. Han, "Pinolenic acid downregulates lipid anabolic pathway in HepG2 cells," *Lipids*, vol. 51, no. 7, pp. 847–855, 2016.

[15] Y. Zhao, S. Liu, Z. Sheng et al., "Effect of pinolenic acid on oxidative stress injury in HepG2 cells induced by H_2O_2," *Food Science and Nutrition*, vol. 9, no. 10, pp. 5689–5697, 2021.

[16] R. Takala, D. P. Ramji, and E. Choy, "The beneficial effects of pine nuts and its major fatty acid, pinolenic acid, on inflammation and metabolic perturbations in inflammatory disorders," *International Journal of Molecular Sciences*, vol. 24, no. 2, p. 1171, 2023.

[17] A. Lahlou, S. Lyashenko, T. Chileh-Chelh et al., "Fatty acid profiling in the genus Pinus in relation to its chemotaxonomy and nutritional or pharmaceutical properties," *Phytochemistry*, vol. 206, Article ID 113517, 2023.

[18] S. Kim, J. Chen, T. Cheng et al., "PubChem 2019 update: improved access to chemical data," *Nucleic Acids Research*, vol. 47, no. D1, pp. D1102–D1109, 2019.

[19] A. Daina, O. Michielin, and V. Zoete, "SwissTargetPrediction: updated data and new features for efficient prediction of protein targets of small molecules," *Nucleic Acids Research*, vol. 47, no. W1, pp. W357–W364, 2019.

[20] G. Stelzer, N. Rosen, I. Plaschkes et al., "The GeneCards suite: from gene data mining to disease genome sequence analyses," *Current Protocols in Bioinformatics*, vol. 54, pp. 1.30.1–1.30.33, 2016.

[21] J. S. Amberger, C. A. Bocchini, F. Schiettecatte, A. F. Scott, and A. Hamosh, "OMIM.org: online Mendelian Inheritance in Man (OMIM®), an online catalog of human genes and genetic disorders," *Nucleic Acids Research*, vol. 43, no. D1, pp. D789–D798, 2015.

[22] D. S. Wishart, Y. D. Feunang, A. C. Guo et al., "DrugBank 5.0: a major update to the DrugBank database for 2018," *Nucleic Acids Research*, vol. 46, no. D1, pp. D1074–D1082, 2018.

[23] N. Li, Q. Pang, Y. Zhang et al., "Ginsenoside ompound K reduces neuronal damage and improves neuronal synaptic dysfunction by targeting Aβ," *Frontiers in Pharmacology*, vol. 14, Article ID 1103012, 2023.

[24] Y. F. Wang, Y. Y. Chang, X. M. Zhang et al., "Salidroside protects against osteoporosis in ovariectomized rats by inhibiting oxidative stress and promoting osteogenesis via Nrf2 activation," *Phytomedicine*, vol. 99, Article ID 154020, 2022.

[25] K. Kostov, "The causal relationship between endothelin-1 and hypertension: focusing on endothelial dysfunction, arterial stiffness, vascular remodeling, and blood pressure regulation," *Life*, vol. 11, no. 9, p. 986, 2021.

[26] R. Mei, M. Wu, and F. Ren, "Knockdown of circ_0002194 protects against oxidized low-density lipoprotein-induced cell damage via the regulation of the miR-637/PACS2 axis in human vascular endothelial cells," *Interactive Cardiovascular and Thoracic Surgery*, vol. 35, no. 4, Article ID ivac210, 2022.

[27] Z. Shi, J. Yao, X. Ma, D. Xu, and G. Ming, "CUL5-mediated visfatin (NAMPT) degradation blocks endothelial proliferation and angiogenesis via the MAPK/PI3K-AKT signaling," *Journal of Cardiovascular Pharmacology*, vol. 78, no. 6, pp. 891–899, 2021.

[28] B. Burja, T. Kuret, T. Janko et al., "Olive leaf extract attenuates inflammatory activation and DNA damage in human arterial endothelial cells," *Frontiers in Cardiovascular Medicine*, vol. 6, p. 56, 2019.

[29] Y. Shen, B. Zhang, X. Pang et al., "Network pharmacology-based analysis of xiao-xu-ming decoction on the treatment of alzheimer's disease," *Frontiers in Pharmacology*, vol. 11, Article ID 595254, 2020.

[30] P. Gong, X. Wang, M. Liu et al., "Hypoglycemic effect of a novel polysaccharide from Lentinus edodes on STZ-induced diabetic mice via metabolomics study and Nrf2/HO-1 pathway," *Food and Function*, vol. 13, no. 5, pp. 3036–3049, 2022.

[31] T. Liu, X. Tang, Y. Cui et al., "Fibroblast growth factor 19 improves LPS-induced lipid disorder and organ injury by regulating metabolomic characteristics in mice," *Oxidative Medicine and Cellular Longevity*, vol. 2022, Article ID 9673512, 19 pages, 2022.

[32] B. Richter, J. Haller, D. Haffner, and M. Leifheit-Nestler, "Klotho modulates FGF23-mediated NO synthesis and oxidative stress in human coronary artery endothelial cells," *Pfluegers Archiv European Journal of Physiology*, vol. 468, no. 9, pp. 1621–1635, 2016.

[33] C. Angolano, E. Kaczmarek, S. Essayagh et al., "A20/TNFAIP3 increases ENOS expression in an ERK5/KLF2-dependent manner to support endothelial cell health in the face of inflammation," *Frontiers in Cardiovascular Medicine*, vol. 8, Article ID 651230, 2021.

[34] O. Levy-Ontman, M. Huleihel, R. Hamias, T. Wolak, and E. Paran, "An anti-inflammatory effect of red microalga polysaccharides in coronary artery endothelial cells," *Atherosclerosis*, vol. 264, pp. 11–18, 2017.

[35] I. Sato, S. Yamamoto, M. Kakimoto et al., "Suppression of nitric oxide synthase aggravates non-alcoholic steatohepatitis and atherosclerosis in SHRSP5/Dmcr rat via acceleration of abnormal lipid metabolism," *Pharmacological Reports*, vol. 74, no. 4, pp. 669–683, 2022.

[36] Z. Liu, B. Shi, Y. Wang et al., "Curcumin alleviates aristolochic acid nephropathy based on SIRT1/Nrf2/HO-1 signaling pathway," *Toxicology*, vol. 479, Article ID 153297, 2022.

[37] S. S. Ndlovu, A. A. Chuturgoon, and T. Ghazi, "Moringa oleifera Lam Leaf extract stimulates NRF2 and attenuates ARV-induced toxicity in human liver cells (HepG2)," *Plants*, vol. 12, no. 7, p. 1541, 2023.

[38] M. A. Memon, Y. Wang, T. Xu et al., "Lipopolysaccharide induces oxidative stress by triggering MAPK and Nrf2 signalling pathways in mammary glands of dairy cows fed a high-concentrate diet," *Microbial Pathogenesis*, vol. 128, pp. 268–275, 2019.

[39] W. Kuan-Hong and L. Bai-Zhou, "Plumbagin protects against hydrogen peroxide-induced neurotoxicity by modulating NF-κB and Nrf-2," *Archives of Medical Science*, vol. 14, no. 5, pp. 1112–1118, 2018.

[40] Á. Bustamante-Sánchez, J. F. Tornero-Aguilera, V. E. Fernández-Elías, A. J. Hormeño-Holgado, A. A. Dalamitros, and V. J. Clemente-Suárez, "Effect of stress on autonomic and cardiovascular systems in military population: a systematic review," *Cardiology Research and Practice*, vol. 2020, Article ID 7986249, 9 pages, 2020.

[41] Z. Li, X. Gong, D. Li, X. Yang, Q. Shi, and X. Ju, "Intratracheal transplantation of amnion-derived mesenchymal stem cells ameliorates hyperoxia-induced neonatal hyperoxic lung injury via aminoacyl-peptide hydrolase," *International Journal of Stem Cells*, vol. 13, no. 2, pp. 221–236, 2020.

[42] J. N. Asiwe, T. A. Kolawole, B. Ben-Azu et al., "Up-regulation of B-cell lymphoma factor-2 expression, inhibition of oxidative stress and down-regulation of pro-inflammatory cytokines are involved in the protective effect of cabbage (*Brassica oleracea*) juice in lead-induced endothelial dysfunction in rats," *Journal of Trace Elements in Medicine and Biology*, vol. 73, Article ID 127014, 2022.

[43] M. Song, L. Meng, X. Liu, and Y. Yang, "Feprazone prevents free fatty acid (FFA)-induced endothelial inflammation by mitigating the activation of the TLR4/MyD88/NF-κB pathway," *ACS Omega*, vol. 6, no. 7, pp. 4850–4856, 2021.

[44] Z. H. Yang, K. Nill, Y. Takechi-Haraya et al., "Differential effect of dietary supplementation with a soybean oil enriched in oleic acid versus linoleic acid on plasma lipids and atherosclerosis in LDLR-deficient mice," *International Journal of Molecular Sciences*, vol. 23, no. 15, p. 8385, 2022.

[45] Y. Zhou, H. Khan, J. Xiao, and W. S. Cheang, "Effects of arachidonic acid metabolites on cardiovascular health and disease," *International Journal of Molecular Sciences*, vol. 22, no. 21, Article ID 12029, 2021.

[46] V. S. Shramko, E. V. Striukova, Y. V. Polonskaya et al., "Associations of antioxidant enzymes with the concentration of fatty acids in the blood of men with coronary artery atherosclerosis," *Journal of Personalized Medicine*, vol. 11, no. 12, p. 1281, 2021.

[47] X. Wang, L. Zhang, W. Sun et al., "Changes of metabolites in acute ischemic stroke and its subtypes," *Frontiers in Neuroscience*, vol. 14, Article ID 580929, 2020.

[48] S. C. R. Sherratt, P. Libby, D. L. Bhatt, and R. P. Mason, "A biological rationale for the disparate effects of omega-3 fatty acids on cardiovascular disease outcomes," *Prostaglandins, Leukotrienes and Essential Fatty Acids*, vol. 182, Article ID 102450, 2022.

[49] X. Lin, L. Lécuyer, X. Liu et al., "Plasma metabolomics for discovery of early metabolic markers of prostate cancer based on ultra-high-performance liquid chromatography-high

resolution mass spectrometry," *Cancers*, vol. 13, no. 13, p. 3140, 2021.

[50] S. S. Mohan, X. D. Ping, F. L. Harris, N. J. Ronda, L. A. Brown, and T. W. Gauthier, "Fatty acid ethyl esters disrupt neonatal alveolar macrophage mitochondria and derange cellular functioning," *Alcoholism: Clinical and Experimental Research*, vol. 39, no. 3, pp. 434–444, 2015.

[51] N. R. Patel, S. Hatziantoniou, A. Georgopoulos et al., "Mitochondria-targeted liposomes improve the apoptotic and cytotoxic action of sclareol," *Journal of Liposome Research*, vol. 20, no. 3, pp. 244–249, 2010.

[52] H. J. Fan, C. H. Wang, B. G. Hsu, and J. P. Tsai, "Association between serum adipocyte fatty acid binding protein level and endothelial dysfunction in chronic hemodialysis patients," *Life*, vol. 12, no. 2, p. 316, 2022.

[53] A. Minenkova, E. E. W. Jansen, J. Cameron et al., "Is impaired energy production a novel insight into the pathogenesis of pyridoxine-dependent epilepsy due to biallelic variants in ALDH7A1?" *PLoS One*, vol. 16, no. 9, Article ID e0257073, 2021.

[54] J. Kalucka, L. Bierhansl, N. V. Conchinha et al., "Quiescent endothelial cells upregulate fatty acid β-oxidation for vasculoprotection via redox homeostasis," *Cell Metabolism*, vol. 28, no. 6, pp. 881–894.e13, 2018.

[55] Y. Kang, Y. Song, Y. Luo et al., "Exosomes derived from human umbilical cord mesenchymal stem cells ameliorate experimental non-alcoholic steatohepatitis via Nrf2/NQO-1 pathway," *Free Radical Biology and Medicine*, vol. 192, pp. 25–36, 2022.

[56] Z. Cao, J. Pan, X. Sui et al., "Protective effects of Huangqi Shengmai yin on Type 1 diabetes-induced cardiomyopathy by improving myocardial lipid metabolism," *Evidence-based Complementary and Alternative Medicine*, vol. 2021, pp. 1–13, 2021.

[57] D. Luo, X. Dong, J. Huang, C. Huang, G. Fang, and Y. Huang, "Pueraria lobata root polysaccharide alleviates glucose and lipid metabolic dysfunction in diabetic db/db mice," *Pharmaceutical Biology*, vol. 59, no. 1, pp. 380–388, 2021.

[58] R. Mallick and A. K. Duttaroy, "Modulation of endothelium function by fatty acids," *Molecular and Cellular Biochemistry*, vol. 477, no. 1, pp. 15–38, 2022.